Reconstruction of dispersion curves in the frequency-wavenumber domain using compressed sensing on a random array

Angélique Drémeau, Florent Le Courtois and Julien Bonnel

ENSTA Bretagne and Lab-STICC (UMR CNRS 6285)

2 rue François Verny, 29806 Brest Cedex 9, France

Running title: reconstruction of dispersion curves using compressed sensing

Abstract

In underwater acoustics, shallow water environments act as modal dispersive waveguides when considering low-frequency sources, and propagation can be described by modal theory. In this context, propagated signals are composed of few modal components, each of them propagating according to its own wavenumber. Wavenumber-frequency ($f - k$) representations are classical methods allowing modal separation. However they require large horizontal line sensor arrays aligned with the source. In this paper, to reduce the number of sensors, a sparse model is proposed and combined with prior knowledge on the wavenumber physics. The method resorts to a state-of-the-art Bayesian algorithm exploiting a Bernoulli-Gaussian model. The latter, well-suited to the sparse representations, makes possible a natural integration of prior information through a wise choice of the Bernoulli parameters. The performance of the method is quantified on simulated data and finally assessed through a successful application on real data.

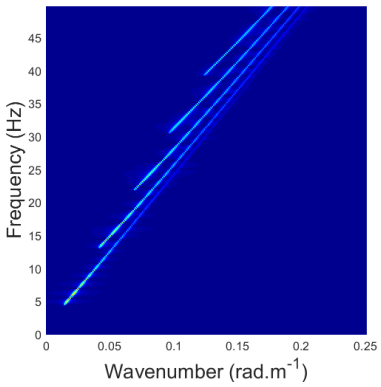

Figure 1: Illustration of a $f - k$ plane obtained within configuration setup exposed in section 4.1 using 240 sensors.

1 Introduction

When considering shallow-water zones and low frequency sound propagation, the sound field is described by a sum of few dispersive modes. In this context, matched mode processing [1] constitutes a relevant approach to infer the properties of the environment [2]. To be effective, this processing requires estimating the modes from the data with a great accuracy.

This modal estimation step has been studied considering various configurations. The most classical one is modal filtering using vertical line arrays (VLA) [3, 4] but other receiver setups have also been addressed as horizontal line arrays (HLA) or single hydrophones. In the case of single hydrophones, we can distinguish two different situations. If the source is motionless, then the modes can be separated using time-frequency processing when the range is large enough [5], and non-linear signal processing when

the range gets smaller [6, 7]. If the source is moving, then synthetic horizontal aperture may be formed to resolve mode interferences [8, 9] or modal wavenumbers [10, 11]. True horizontal aperture is directly provided by HLAs. Essentially, if the acoustic field can be sampled in the range (i.e. horizontal) dimension, then the mode estimation procedure is equivalent to a spectral estimation problem. As a result, considering a long HLA and a monochromatic source at the endfire position, the wavenumber spectrum can be obtained by applying a Fourier transform in the array dimension [12, 13]. In this paper, we propose a new method for wavenumber spectrum estimation in the context of short HLAs and broadband sources. Our work is particularized to shallow water environments and low frequencies. In addition, we assume the environment to be range independent, and /or varying slowly so that mode coupling can be neglected.

In the following, spatial Fourier transform will be denoted SFT. It transforms signals from the spatial to the wavenumber domain. The notation TFT will be reserved for the (more classical) temporal Fourier transform, which transforms signals from the time domain to the frequency domain. The representation associated to the wavenumber domain will always be refered to as the *wavenumber spectrum*, while the representation associated to the frequency domain will always be referred to as the *spectrum*.

Wavenumber spectrum estimation using SFT does not present any theoretical difficulty. However, it suffers from the classical drawbacks of the TFT. A large aperture is required to obtain a decent resolution and the hydrophone spacing must be small

enough to prevent aliasing. Because of these two restrictions, extremely large HLAs are required to resolve the modes in underwater acoustics using SFT. However, this issue may be circumvented by resorting to more advanced spectral estimation methods. Among them, High Resolution (HR) methods are known to be more accurate than the SFT. When using the same number of measurements, HR methods allow a better separation of nearby spectral components [14]. Applications of HR methods in underwater acoustics for modal separation have been proposed using auto-regressive models [15, 16, 17, 18] and subspace separation methods [19, 20].

Since the propagation in shallow-water environments is described by a small number of modes, the consideration of sparse models constitutes a promising alternative to HR methods. Developments in signal processing have raised the interest of compressed sensing (CS) methods for an accurate sampling and reconstruction of sparse signals [21]. CS methods have met many applications in underwater acoustics [22, 23], and for imaging the modal dispersion of surface waves [24]. A first application of CS to estimate modal spectrum in underwater acoustics has been proposed in [25].

When considering a broadband source, wavenumber spectra can be estimated at each of the source frequencies. The concatenation of them results in a frequency-wavenumber ($f - k$) diagram (see Fig. 1), representative of the waveguide dispersion [12, 13, 25]. As a consequence, $f-k$ diagram constructions suffer from the drawbacks inherited from each wavenumber spectrum estimation. To partially solve this problem,

Le Courtois and Bonnel have proposed in [26] a post-processing method to track the wavenumbers in badly resolved $f-k$ diagrams. Tracking is performed using particle filtering (PF) [27]. To do so, the wavenumber spectrum (at a given frequency) is modeled as a dynamic system parametrized by two equations: a system equation and an observation equation. The observation equation is the equation that allows generating a wavenumber spectrum if the (discrete) wavenumbers are known. On the other hand, the system equation is an iterative relation linking the wavenumbers from one frequency to another. This system equation thus benefits from a physical hypothesis on the wavenumber dispersion in the frequency dimension, and such an idea will also be used in our paper. Note that the PF method is particularly interesting when the number of sensors is too small to separate the modes. However, the number of propagating modes must be known a priori to initiate the tracking operation. In addition, the resolution of the method depends on the distribution of the particles and cannot be easily estimated. These last two constraints will be eased in the present paper.

This paper introduces a framework relying on the hypothesis that the propagation is sparse (in the wavenumber dimension) and dispersive (in the frequency dimension). A methodology allowing $f-k$ estimation and integrating these two physical hypotheses is presented. To this end, the work focuses on the sparse estimation of the wavenumber spectrum using a Bernoulli-Gaussian model [28]. In this framework, each wavenumber spectrum is a sparse vector. Each wavenumber bin is supposed to be "on" (*i.e.,*

there is a mode propagating at this particular wavenumber value) or "off" (*i.e.,* there is no mode propagating at this particular wavenumber value) according to a Bernouilli distribution. Once a wavenumber bin is "on", the corresponding mode amplitude is supposed to follow a Gaussian distribution. In this approach, the Bernoulli parameter offers a great opportunity to take into account the dispersive propagation, so that the sparse wavenumber spectra estimated at each frequency are naturally related with each other. In this paper, the Soft Bayesian Pursuit algorithm [29] (SoBaP) is considered to efficiently perform the estimation procedure.

The paper is organized as follows. The second section recalls the physical principles of the modal propagation and the prior knowledge exploited to build up the $f-k$ representation. The third section is dedicated to a mathematical formulation of the problem and the integration of the physical prior. Finally, in section 4, the method is applied to synthetic simulations and to marine data recorded in the North Sea.

2 Acoustic propagation in dispersive shallow water environments

2.1 Received signal

In shallow-water environments, the acoustic propagation is described by the modal theory. The propagation depends on the frequency f and is qualified as dispersive. When considering an emitting source $s(f)$ at depth z_s, the received signal on a sensor

located at the distance r and depth z can be written as [30]

$$y(f,r) = Q\,\frac{s(f)}{\sqrt{r}}\sum_{m=1}^{M(f)}\psi_m(f,z_s)\;\psi_m(f,z)\;\frac{e^{-jrk_{rm}(f)}}{\sqrt{k_{rm}(f)}} + w(f,r), \tag{1}$$

where Q is a constant factor, $M(f)$ is the number of propagating modes at frequency f, $k_{rm}(f)$ is the horizontal wavenumber of the m^{th} mode and $\psi_m(f,z)$ is the modal depth function of the m^{th} mode. The quantity $w(f,r)$ stands for the TFT of the noise attached to the measurements. Note that, for the sake of clarity, we deliberately omit here the dependence in z in the notation of $y(f,r)$ and $w(f,r)$ as we will consider HLAs, *i.e.,* sensors at a constant depth.

For subsequent convenience, we define the amplitude of the m^{th} mode as

$$A_m(f) \triangleq \frac{\psi_m(f,z_s)\;\psi_m(f,z)}{\sqrt{k_{rm}(f)}}, \tag{2}$$

so that Eq. (1) can finally be re-expressed as

$$y(f,r) = Q\,\frac{s(f)}{\sqrt{r}}\sum_{m=1}^{M(f)}A_m(f)\;e^{-jrk_{rm}(f)} + w(f,r). \tag{3}$$

Considering a HLA of regularly spaced sensors aligned with the source (endfire position), the ℓ^{th} sensor is at a distance of $r = (\ell-1)\Delta_r + r_0$ from the source, where r_0 is the distance of the first sensor and Δ_r the sensor spacing. In this paper, we assume a distant source (so that $r_0 \gg \Delta_r$). Under this assumption, the geometrical attenuation factor $1/\sqrt{r}$ can be considered as constant over the entire sensor array. Similarly, we will neglect any eventual modal attenuation, so that the modal wavenumber $k_{rm}(f)$ may be considered as real numbers.

As stated in the introduction, considering a monochromatic source, the wavenumber spectrum can be estimated by performing a simple SFT along the HLA. If a broadband source is available, a $f-k$ diagram can be obtained by concatenating the wavenumber spectra at several frequencies [12]. However, this requires a long and dense HLA. The goal of this paper is to estimate $f-k$ diagram in less constrained contexts, in particular when the number of sensors is low.

2.2 Dispersion relation

In waveguides, the horizontal wavenumbers k_{rm} are linked to their vertical counterparts k_{zm} by the dispersion relation, that is, for a given frequency f,

$$\left(\frac{2\pi f}{c}\right)^2 = k_{rm}(f)^2 + k_{zm}(f)^2, \tag{4}$$

where c is the speed of the sound[1].

Discretizing the frequency axis (with $f = \nu\Delta_f$, $\nu \in \mathbb{N}$) and denoting $k_{rm}[\nu] = k_{rm}(\nu\Delta_f)$, the wavenumbers attached to two successive indices are then defined as [25]

$$k_{rm}[\nu+1]^2 = k_{rm}[\nu]^2 + (2\nu+1)\left(\frac{2\pi\Delta_f}{c}\right)^2 + \epsilon[\nu], \tag{5}$$

where Δ_f is the sampling period, *i.e.,* the step between two frequency bins, and $\epsilon[\nu] = k_{zm}[\nu]^2 - k_{zm}[\nu+1]^2$. In shallow-water environments, the vertical wavenumbers k_{zm}

[1]Note that the quantities c and $k_{zm}(f)$ are depth-dependent. Here again, we choose to skip this dependence in the expression as it will be considered as constant in our sensing context. As we will see in the following, the way the dispersion relation will be exploited in the proposed approach allows some deviations from this assumption.

weakly depend on the frequency [30]; the quantity ϵ is smaller than the other terms of the equation and can be neglected. This approximation may not be true when the propagation becomes strongly range dependent. This case will not be considered in the remainder of the paper.

Equation (5) expresses the dispersive nature of the wavenumbers in a shallow-water environment. In this paper, we propose to take into account this physical information in the reconstruction procedure of the $f - k$ diagram. Note that Eq. (5) was used in [26, 25] to post-process badly resolved $f - k$ diagrams. In this paper, Eq. (5) will be embedded as a prior information into a Bayesian CS algorithm, allowing a direct estimation of the $f - k$ diagram.

3 Compressed sensing

When dealing with compressed sensing, two properties have to be verified:

- *sparsity*: the signal to be acquired can be represented with a few non-zero elements in a given representation basis,
- *incoherence*: the sensing must be made in a domain "as orthogonal as possible" to the representation basis.

Under these conditions, the theory of compressed sensing guarantees that we can recover the signal from a number of samples of the order of the number of its non-zero elements in the representation basis.

In words, "incoherence" expresses the fact that a signal admitting a sparse representation in a particular domain (for example, in the frequency domain) must be acquired in the domain where its representation is spread out (for example, the time domain). In the time-frequency example, the sensing domain is the canonical basis (time) and the sparsity domain is the Fourier basis (frequency).

The reconstruction problem of the $f-k$ diagram is then a perfect application case for compressed sensing: the signal of interest is sparse in the wavenumber domain (only few wavenumbers propagate in shallow water environments and at low frequencies), and is acquired in the spatial domain. From a mathematical point of view, this means that we acquire the signal in the canonical basis (space, through the sensor array) and the sparsity domain is the spatial Fourier basis (wavenumber). We refer the reader to [31] for a brief introduction to compressed sensing, or to [32] for more insights.

3.1 State of the art

Formally, let $\mathbf{y}_\nu \in \mathbb{C}^L$ be the signal measured over the L sensors at the frequency index ν. Adopting a discretized matrix formulation, Eq. (3) can be re-expressed as

$$\mathbf{y}_\nu = \mathbf{D}\mathbf{z}_\nu + \mathbf{w}_\nu, \tag{6}$$

where $\mathbf{D}$ is a $(L \times N)$-dictionary of Fourier discrete atoms, namely whose (ℓ, n)-element is $d_{nl} \triangleq e^{-j2\pi \frac{nl}{N}}$, and $\mathbf{z}_\nu = [z_{\nu,1}, \ldots, z_{\nu,N}]^T \in \mathbb{C}^N$ is the wavenumber spectrum at the frequency index, *i.e.,* the ν^{th} transposed line of the $f-k$ diagram to

estimate.

Then, N corresponds to the number of discretized points in the horizontal wavenumber domain, say

$$\kappa_{rn} \triangleq 2\pi \frac{n}{N\Delta_r}, \quad \forall n \in \{1, \ldots, N\}, \tag{7}$$

and $\mathbf{z}_\nu$ gathers the amplitudes attached to each of the wavenumber bins.

According to the modal theory in shallow water environments and at low frequencies, we have $M[\nu] \ll N$ (see Eq. (3)), where $M[\nu] = M(\nu\Delta_f)$. In other words, the vector $\mathbf{z}_\nu$ has few non-zero elements, corresponding to the propagating modal wavenumbers. Formally, we define by $\mathcal{M}_\nu \subset \{1, \ldots, N\}$ the set of cardinality $M[\nu]$ gathering the indices of the propagating wavenumbers. For each of the $M[\nu]$ propagating modes, there exists $n \in \mathcal{M}_\nu$ such as,

$$k_{rm}[\nu] = \kappa_{rn} \qquad \text{and} \qquad A_m[\nu] = z_{\nu,n}, \tag{8}$$

where $A_m[\nu] = A_m(\nu\Delta_f)$ defined as in Eq. (2).

We note here that the precise estimation of the set $\mathcal{M}_\nu$ is crucial. From it derives the knowledge of the propagating wavenumbers $k_{rm}[\nu]$ and the modal amplitudes $A_m[\nu]$, of particular interest for source depth estimation and/or environmental inversion.

The sparsity of the vector $\mathbf{z}_\nu$ constitutes important information on the $f - k$ diagram, that should be taken into account in the reconstruction procedure. Several formulations of the corresponding sparse recovery problem can then be considered. In

this paper, we focus on the following one:

$$\hat{\mathbf{z}}_\nu = \underset{\mathbf{z}_\nu}{\operatorname{argmin}} \|\mathbf{y}_\nu - \mathbf{D}\mathbf{z}_\nu\|_2^2 + \lambda\|\mathbf{z}_\nu\|_0, \tag{9}$$

where $\|\mathbf{z}_\nu\|_0$ stands for the ℓ_0 pseudo-norm of $\mathbf{z}_\nu$ (counting the number of non-zero elements in $\mathbf{z}_\nu$) and λ is a parameter specifying the trade-off between the sparsity constraint and the data-fidelity term $\|\mathbf{y}_\nu - \mathbf{D}\mathbf{z}_\nu\|_2^2$. The solution of Eq. (9) can be naturally interpreted as the least-square (LS) solution (which, in our case, is equivalent to a SFT when $\mathbf{y}_\nu$ is uniformly sampled) penalized by the sparsity of the solution.

Solving Eq. (9) is an NP-hard problem [33], *i.e.,* it generally requires a combinatorial search over the entire solution space. Therefore, heuristic (but tractable) algorithms have been devised to deal with this problem. We can roughly divide them into three families: *i) the greedy algorithms* (*e.g.,* [34, 35]) which build up the sparse solution by making a succession of greedy decisions, *ii) the relaxation-based algorithms* (*e.g.,* [36, 37]) which replace the ℓ_0 pseudo-norm by some ℓ_p-norm (with $p \in]0, 1]$) leading to a relaxed problem efficiently solvable by standard optimization procedures, *iii) the Bayesian algorithms* (*e.g.,* [38, 29, 39]) which express the problem as the solution of a Bayesian inference problem and apply statistical tools to solve it.

The Bayesian approaches are particularly suitable when the noise level is not known. In addition, they offer a simple framework to implement any prior information available on the physical context of the problem. In our case, they present in particular a

great opportunity to take into account the dispersion relation given in Eq. (5).

3.2 Bayesian formulation

Let us first assume $\mathbf{w}_\nu$ in Eq. (6) to be a circular Gaussian noise (denoted by $\mathcal{CN}$) with zero mean and variance σ_w^2. We suppose then that $\mathbf{z}_\nu$ is the realization of a Bernoulli-Gaussian (BG) model [29], that is

$$\mathbf{z}_\nu = \mathbf{s}_\nu \odot \mathbf{x}_\nu, \tag{10}$$

where $\odot$ represents here the term-by-term product, and

$$p(\mathbf{s}_\nu) = \prod_{n=1}^{N} p(s_{\nu,n}) \quad \text{with} \quad p(s_{\nu,n}) = \text{Ber}(p_{\nu,n}), \tag{11}$$

$$p(\mathbf{x}_\nu) = \prod_{n=1}^{N} p(x_{\nu,n}) \quad \text{with} \quad p(x_{\nu,n}) = \mathcal{CN}(0, \sigma_x^2). \tag{12}$$

The Bernoulli distribution (denoted by Ber in the equation above) has a realization domain on $\{0, 1\}$ and depends on a parameter $p_{\nu,n}$ which represents the probability of being equal to 1. The circular Gaussian distribution put on the variable $\mathbf{x}_\nu$ is assumed to be with zero mean and variance σ_x^2.

With words, $\mathbf{s}_\nu$ is called the *support* of the sparse representation. It is such as $\mathbf{s}_\nu \in \{0, 1\}^N$. Every $1-$value in $\mathbf{s}_\nu$ indicates a wavenumber bin corresponding to a propagating modal wavenumber; every $0-$value in $\mathbf{s}_\nu$ indicates a wavenumber bin corresponding to a wavenumber that does not propagate. The quantity $\mathbf{x}_\nu$ stands for the *amplitude* of the sparse representation. Coming back to Eq. (8), $\mathbf{s}_\nu$ serves then to define

the set $\mathcal{M}_\nu$ of the wavenumber bins corresponding to the propagating wavenumbers

$$\mathcal{M}_\nu = \Big\{ n \in \{1, \dots, N\} | s_{\nu,n} = 1 \Big\},$$

while $\mathbf{x}_\nu$ can be directly linked to the amplitudes $A_m[\nu]$ of the propagating modes. As a consequence, the latter are assumed to be independently and identically distributed according to a Gaussian law, as expressed in Eq. (12).

Formally, the BG model (11)-(12) is well-suited to modelling situations where $\mathbf{y}_\nu$ stems from a sparse process: if $p_{\nu,n} \ll 1$, $\forall n$, only a small number of $s_{\nu,n}$'s will typically be non-zero, *i.e.,* the observations $\mathbf{y}_\nu$ will be generated with high probability from a small subset of the columns of $\mathbf{D}$. More rigorously, it has been proved (see [28, 40]) that, within model (11)-(12), the joint Maximum A Posteriori estimation problem shares the same set of solutions as the standard sparse recovery problem (9). This connection gives weight to the general use of this model in sparse recovery problems.

In this paper, we choose to resort to a particular algorithm of the sparsity literature, that is the Soft Bayesian Pursuit algorithm (SoBaP) [29]. Exploiting model (6)-(12), SoBaP aims at solving the following marginalized MAP problem

$$\hat{\mathbf{s}}_\nu = \underset{\mathbf{s}_\nu}{\operatorname{argmax}}\, p(\mathbf{s}_\nu | \mathbf{y}_\nu), \tag{13}$$

where

$$p(\mathbf{s}_\nu | \mathbf{y}_\nu) = \int_{\mathbf{x}_\nu} p(\mathbf{s}_\nu, \mathbf{x}_\nu | \mathbf{y}_\nu) d\mathbf{x}_\nu. \tag{14}$$

The algorithm relies on a variational approximation [41] which constitutes the building block of the current state-of-the-art algorithms [42].

Once $\mathbf{s}_\nu$ is estimated, the amplitudes of the propagated wavenumbers can be computed by a simple pseudo-inversion of the dictionary $\mathbf{D}$, restricted to its non-zero columns, say $\mathbf{D}_{\hat{\mathbf{s}}_\nu}$

$$\hat{\mathbf{x}}_\nu = \mathbf{D}^+_{\hat{\mathbf{s}}_\nu} \mathbf{y}_\nu \tag{15}$$

where $^+$ stands for the pseudo-inverse operator.

3.3 Incorporating a priori information about dispersive propagation

In our application context, the BG model presents an additional advantage: relying on the dedicated support variable $\mathbf{s}_\nu$, it allows for an easy implementation of *a priori* information through the Bernoulli parameters $p_{\nu,n}$ (see Eq. (11)).

By the physical relation (5), the wavenumbers estimated at the frequency ν define an *a priori* on the wavenumbers at the next frequency $\nu + 1$. Consequently, the sparse representation support can be propagated to the $\nu + 1$. This can be done by means of the Bernoulli parameters $p_{\nu+1,n}$ which set the probabilities for the elements in $\mathbf{s}_{\nu+1}$ to be set to 1 (*i.e.,* for the wavenumbers to be chosen). Formally, we fix, for all $n \in \{1, \ldots, N\}$,

$$p_{\nu+1,n} = \begin{cases} 0.7 & \text{if} \quad n \in \mathcal{I}_\nu, \\ 0.3 & \text{if} \quad (n-1) \in \mathcal{I}_\nu, \\ 0.3 & \text{if} \quad (n+1) \in \mathcal{I}_\nu, \\ M[\nu+1]/N & \text{otherwise} \end{cases} \tag{16}$$

with

$$\mathcal{I}_\nu = \left\{ n \;\middle|\; n = \left[\sqrt{n'^2 + (2\nu+1)\left(\frac{N\Delta_r\Delta_f}{c}\right)^2} \right],\ \hat{s}_{\nu,n'} = 1 \right\}, \tag{17}$$

where $[.]$ is the nearest natural number. We explain these equations hereafter.

The expression (17) is directly derived from Eq. (5), where we have replaced the wavenumbers $k_{rm}[\nu+1]$ and $k_{rm}[\nu]$ by their discretized expressions (7), introducing indices n and n' (see Eq. (8)). To make it clear, let us assume that at frequency ν, a mode propagates at the wavenumber bin n', *i.e.,* $\hat{s}_{\nu,n'} = 1$. Then, Eq. (5) allows to predict the wavenumber value at frequency $\nu+1$. The corresponding wavenumber bin is the index n given by Eq. (17). As a result, a weight of 0.7 is given to the bin n predicted at frequency $\nu+1$ (*i.e.,* such that $n \in \mathcal{I}_\nu$). Figure 2 illustrates the procedure.

The round operator $[.]$ in Eq. (17) throws off the unknown quantity $\epsilon[\nu]$ in Eq. (5) which contains the (weak) frequency dependence of the vertical wavenumbers. It is however taken into account in a probabilistic way through the Bernoulli parameters of the nearest neighbors of the indices selected by $\mathcal{I}_\nu$. Then, if a wavenumber is found to propagate at frequency ν and bin n' (*i.e.,* $\hat{s}_{\nu,n'} = 1$), a weight of 0.3 is given to the position $n+1$ and $n-1$ at frequency $\nu+1$ where $n \in \mathcal{I}_\nu$.

Note finally that the numerical values of 0.7 and 0.3 are arbitrarily chosen. The other positions, which have been not predicted by the dispersion relation are assumed to have the same probability to be chosen, equal to $M[\nu+1]/N$.

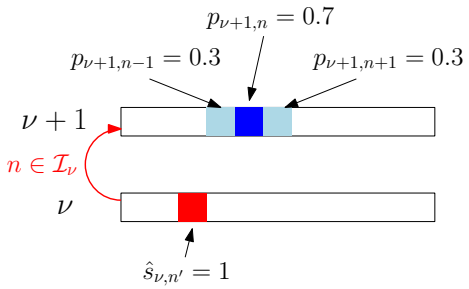

Figure 2: Illustration of the definition of the Bernoulli parameters as expressed in (16)-(17), on two successive rows of the $f - k$ diagram.

Interestingly, we note that, by virtue of the flexibility of the Bayesian framework, the value of $M[\nu + 1]$ in Eq. (16) does not have to be precisely known, a rough guess (*e.g.,* within an error of 2 modes) being sufficient to guarantee robust results; here, the knowledge of the number of propagating modes is less essential than in HR and tracking methods. As examples, a strong *a priori* is necessary for the initialization of particle filtering [25], for the choice of the eigenvalues in MUSIC [20] or the order of auto-regressive models as in [16, 18]. Also, the environmental parameters, as the sound speed, may not be perfectly known without impacting the performance of the approach (see experiments with real data in section 4.2). Note that, in cases of strong environmental uncertainties, a simple and straightforward way to insure robustness will be to extend the neighborhood of significative probabilities (indices $n + 1$ and $n - 1$ in (16)) to farther wavenumber bins (for example $n + 2$ and $n - 2$). Doing so, we can compensate the uncertainty over the propagating environment by a more relaxed probabilistic model. Note that the extreme case will be then to set all parameters $p_{\nu+1,n}$

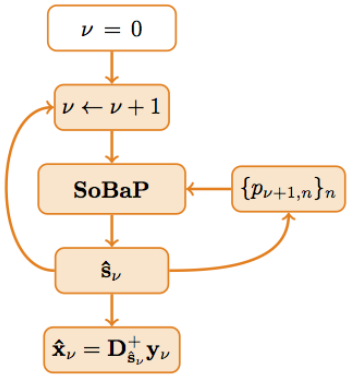

Figure 3: Scheme summarizing the overall proposed methodology for $f - k$ reconstruction.

to a same value, resulting in the standard sparse case, as originally considered in [29].

Fig. 3 illustrates the entire $f - k$ diagram estimation process. Given a frequency index ν of the $f - k$ plane, wavenumbers are estimated by solving the problem (13) using SoBaP. Then Eq. (16) predicts the value of the Bernoulli parameter at the frequency index $\nu + 1$. The frequency is incremented to index $\nu + 1$ and problem (13) is solved using the updated Bernoulli parameters.

4 Applications

In this section, we propose two experimental setups to assess the performance of the proposed method: to quantify the performance, we first consider synthetic experiments, before applying the method on real data.

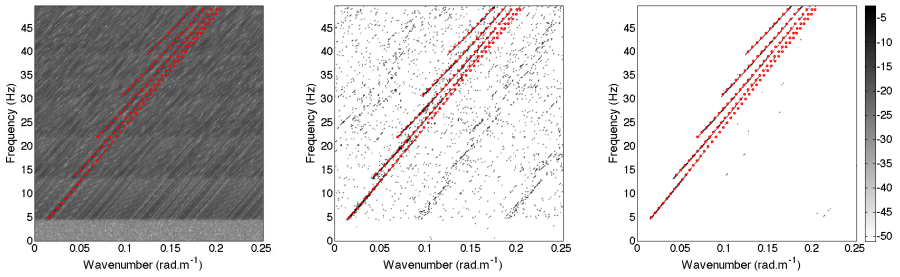

Figure 4: Reconstruction of the dispersion curves (in dB) using measurements from 30 sensors and a signal to noise ratio of 10 dB: (a) LS inversion, (b) OMP, and (c) SoBaP with *dispersive* a priori. The ground truth is represented by red points.

4.1 Simulations

The synthetic data are simulated using a Pekeris waveguide [30]. The water column is assumed to be $D = 130$ m deep with a sound speed $c_{\text{water}} = 1500$ m/s and a density $\rho_{\text{water}} = 1$ kg/m^3. The seabed is a semi-infinite fluid layer with a sound speed of $c_{\text{seabed}} = 2000$ m/s and a density $\rho_{\text{seabed}} = 2$ kg/m^3. The array is composed of 240 hydrophones lying on the seabed and with spacing $\Delta_r = 25$ m, resulting in a 6000 m long antenna. The corresponding spectral resolution of the SFT is then 1.05×10^{-4} rad/m. The source emits a broadband signal between 0 and 50 Hz (corresponding to a white noise or an impulsive signal in the time domain, the latter case was simulated here). The frequency resolution is $\Delta_f = 0.2$ Hz. The source is placed at $D = 130$ m depth to avoid nodes of the modal functions. At 50 Hz, five modes are propagating.

Two sparse representation algorithms are compared for the resolution of the prob-

lem: Orthogonal Matching Pursuit (OMP) [43] as used in [24], and SoBaP incorporating a priori information on the dispersive propagation, as defined earlier. OMP is stopped when $||\mathbf{y}_\nu - \mathbf{D}\hat{\mathbf{x}}_\nu||_2 < \sqrt{L\sigma_w^2}$. SoBaP is stopped when the Kullback-Leibler divergence between the distribution $p(\mathbf{s}, \mathbf{x}|\mathbf{y})$ and its variational approximation is smaller than 10^{-4}. Both algorithms are compared to the least-square (LS) approach, performing a simple inverse Fourier transform.

The resulting $f - k$ diagrams are shown in Fig. 4 together with the ground truth, represented by red points. For all three, 30 sensors are used and a signal-to-noise ratio (SNR) of 10 dB is considered. To account for the CS framework, the positions of the sensors are randomly selected from the 240 simulated measurements. At these settings, the $f - k$ diagram obtained by simple LS inversion and plotted in Fig. 4(a) cannot be correctly interpreted to infer the expected wavenumbers: they do not appear clearly. The one obtained by OMP seems to be more sensitive to noise; some wavenumbers are identified but they have no physical justification. The use of the dispersive *a priori* in SoBaP suppresses all of the artifacts from the $f - k$ plane. These visual results are to be compared with the ground truth, represented by red points on each $f - k$ diagram.

To quantify more precisely the performance of the algorithms, we compute for each of them the normalized Mean Square Error (MSE) between the estimated wavenumbers (corresponding, for each frequency index ν, to the $M[\nu]$ largest coefficients in $\hat{\mathbf{x}}_\nu$) and the true values of the Pekeris model. The error is averaged over the mode number and

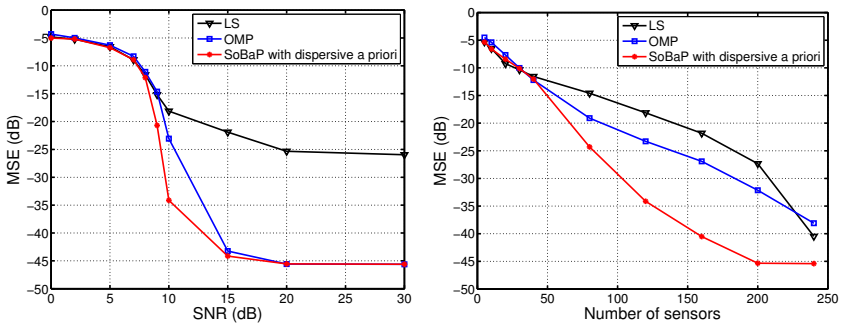

(a) (b)

Figure 5: Normalized Mean Square Error (MSE) on the estimated wavenumbers (in dB) as a function of: (a) the SNR for an array of $L = 120$ sensors and (b) the number of sensors in the array for a SNR of 10 dB.

the frequencies to obtain a global value. The MSE is represented, in Fig. 5(a), as a function of the SNR for a given number of sensors $L = 120$ and in Fig. 5(b), as a function of the number of hydrophones exploited to reconstruct the $f - k$ diagram for a given SNR of 10 dB.

In accordance with previous works [25, 24], both figures illustrate the good behavior of sparse-aware algorithms with regard to naÃ¯ve LS inversion: OMP and the proposed SoBaP procedure outperform the LS estimation in most practical setups, *i.e.,* noisy measurements and few sensors.

As shown in Fig. 5(a), for an SNR greater than 20 dB, the two sparse-aware methods present similar performances, and an exact reconstruction of the wavenumbers is obtained (note that the residual MSE is linked to the resolution of the Fourier matrix $\mathbf{D}$, independently of the number of measurements). The proposed approach proves to

be more interesting in the noisy cases: we thus observe that the SoBaP procedure exploiting the frequency dependence between the wavenumbers shows a faster decrease of the MSE as the SNR increases. For an SNR of 10 dB, the method reaches a MSE around -35 dB, compared to -20 dB for OMP.

This particular setting is considered in more detail in Fig. 5(b), where the performance at SNR$= 10$ dB is assessed from a sensor point of view. Within this setting, the three methods achieve similar (poor) performance for very small numbers of sensors (below $L = 50$). Note that this observation does not contradict the visual interpretation of Fig. 4, as the MSE quantifies the position of the $M[\nu]$ largest estimated wavenumbers without any consideration over false alarms. Beyond 50 sensors, the proposed SoBaP procedure outperforms indisputably the other two approaches.

4.2 North Sea data

In this section, we apply our approach to real data. The considered data was acquired in the North Sea during a seismic campaign led by the Compagnie Générale de Géophysique [44, 45]. The source is an air gun, that is impulsive with a nearly flat spectrum between 0 and 80 Hz. Measurements are performed by a synthetic antenna of 240 ocean-bottom seismometers resting on the seabed. They are spaced at intervals of 25 m, leading to a total length of 6000 m. The pressure field is sampled at 250 Hz. The environment is assumed to be close to a Pekeris waveguide. Within this assumption, the experimental parameters were estimated [45] as: $c_{\text{water}} = 1520$ m/s, $c_{\text{seabed}} = 1875$ m/s,

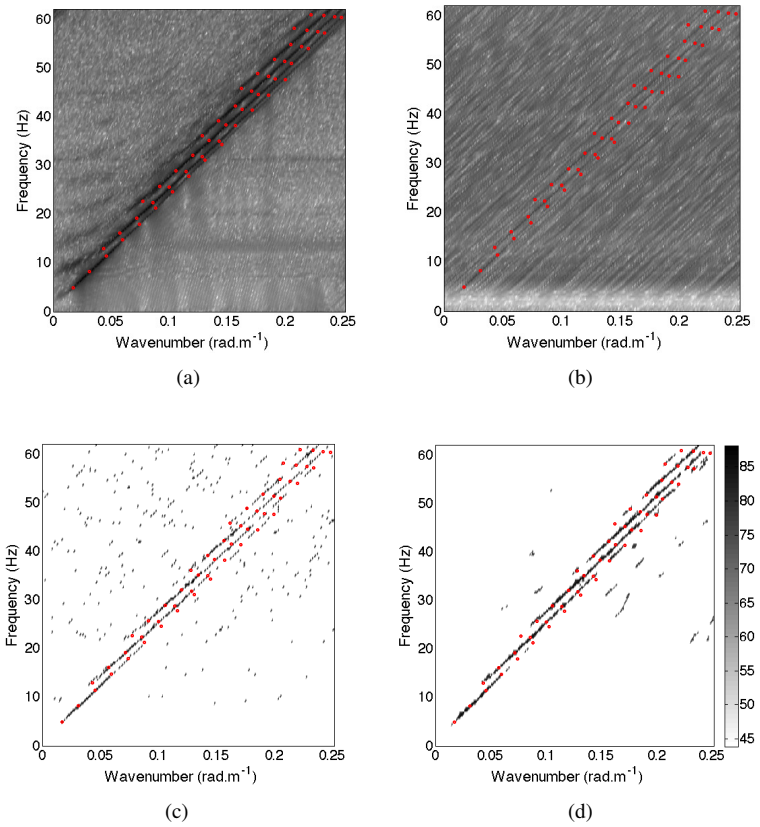

Figure 6: Reconstruction of the dispersion curves (in dB) from the North Sea measurements using: (a) 240 sensors with a LS inversion, (b) 20 sensors with a LS inversion, (c) 20 sensors with the OMP algorithm and (d) 20 sensors with the physics-aware SoBaP algorithm. Red points represent the result of a peak-picking method on the LS inversion on the entire antenna (a).

$D = 130$ m. For this data, we evaluated the SNR around 13 dB.

Fig. 6 presents the $f - k$ representations obtained by the inversion of 20 hydrophones with: (b) a simple LS method, (c) the OMP algorithm and (d) the SoBaP algorithm exploiting the frequency dependence between the wavenumbers. As a comparison, the $f - k$ diagram obtained with a LS inversion using the entire antenna is dis-

played in Fig. 6(a). Moreover, on each figure, we have added in red the wavenumbers selected from the LS inversion on the entire antenna (Fig. 6(a)) using a peak-picking method. These results show the relevance of the proposed approach. We can thus see that sparsity enables an undeniable improvement of the inversion (compared to the simple LS estimate) in particular in terms of noise suppression, but missed (in particular at the highest frequencies) and false detections are still noticeable. Adding a prior knowledge on the propagated wavenumbers allows us to recover perfectly the wavenumbers, even at the highest frequencies (around 60 Hz in our case), while reducing the noise of the $f - k$ diagram.

5 Conclusion

This article deals with the estimation of the wavenumbers in shallow water environments. An array processing method is proposed to reduce the number of the sensors required to separate accurately the wavenumbers over a wide range of frequencies. The proposed method relies on two robust hypotheses. On the one hand, in the wavenumber domain, the wavenumber spectrum is sparse. On the other hand, in the frequency domain, the wavenumber spectra can be related from one frequency to the next using a general dispersion relationship. These two hypotheses call for the utilization of a Bayesian compressed-sensing (CS) algorithm. Indeed, the CS framework is suitable for our sensing context, while the Bayesian framework enables a natural implementa-

tion of the relation linking the wavenumbers from one frequency to the next.

The performance of the proposed method is assessed on simulations. Our algorithm makes possible an accurate wavenumber estimation using a small number of hydrophones, even in noisy contexts. It outperforms other state-of-the-art methods such as Least Square SFT (which does not benefit from any physical hypothesis) and Orthogonal Matching Pursuit (which benefits only from the sparse hypothesis): estimated wavenumbers are more accurate, and the estimated $f - k$ diagrams are globally less noisy. Also, the method is validated on experimental data recorded in the North Sea. In this context, the proposed method performs the estimation of the wavenumbers with a 20-hydrophone HLA.

Because the proposed method is based on CS, it is naturally suitable for cases where the number of measurements (*i.e.,* hydrophones) is small and, ideally, randomly distributed. However, it does not necessarily help in reducing the required range aperture (*i.e.,* the HLA length). As a result, the method may not show its full strength on a small HLA with constant hydrophone spacing. However, interesting perspectives arise for analyzing (existing) synthetic aperture data, where the considered snapshots can be chosen at will along the source/receiver track. Also, the potential of CS should be taken into account when designing new at-sea experiment.

5.1 Acknowledgement

This work have been supported by the DGA/MRIS.

References

[1] T. C. Yang, "Effectiveness of mode filtering: A comparison of matched-field and matched-mode processing," *Journal of Acoustical Society of America*, vol. 87, 1990.

[2] G. Wilson, R. Koch, and P. Vidmar, "Matched mode localization," *The Journal of the Acoustical Society of America*, vol. 84, pp. 310–320, 1988.

[3] J. Buck, J. Preisig, and K. Wage, "A unified framework for mode filtering and the maximum a posteriori mode filter," *The Journal of the Acoustical Society of America*, vol. 103, p. 1813, 1998.

[4] T. Neilsen and E. Westwood, "Extraction of acoustic normal mode depth functions using vertical line array data," *The Journal of the Acoustical Society of America*, vol. 111, pp. 748–756, 2002.

[5] G. Potty, J. Miller, J. Lynch, and K. Smith, "Tomographic inversion for sediment parameters in shallow water," *The Journal of the Acoustical Society of America*, vol. 108, pp. 973–986, 2000.

[6] J. Bonnel, B. Nicolas, J. Mars, and S. Walker, "Estimation of modal group velocities with a single receiver for geoacoustic inversion in shallow water," *The Journal of the Acoustical Society of America*, vol. 128, pp. 719–727, 2010.

[7] J. Bonnel, G. Le Touzé, B. Nicolas, and J. Mars, "Physics-based time-frequency representations for underwater acoustics: Power class utilization with waveguide-invariant approximation," *IEEE Signal Processing Magazine*, vol. 30, no. 6, pp. 120–129, 2013.

[8] C. Gervaise, B. Kinda, J. Bonnel, Y. Stéphan, and S. Vallez, "Passive geoacoustic inversion with a single hydrophone using broadband ship noise," *The Journal of the Acoustical Society of America*, vol. 131, no. 3, pp. 1999–2010, 2012.

[9] Y. Le Gall and J. Bonnel, "Passive estimation of the waveguide invariant per pair of modes," *The Journal of the Acoustical Society of America*, vol. 134, no. 2, pp. EL230–EL236, 2013.

[10] G. Frisk and J. Lynch, "Shallow water waveguide characterization using the Hankel transform," *The Journal of the Acoustical Society of America*, vol. 76, p. 205, 1984.

[11] G. V. Frisk, K. M. Becker, S. D. Rajan, C. J. Sellers, *et al.*, "Modal mapping experiment and geoacoustic inversion using sonobuoys," *IEEE Journal of Oceanic Engineering*, vol. PP, no. 99, pp. 1–14, 2014.

[12] Ö. Yilmaz, *Seismic data analysis: processing, inversion, and interpretation of seismic data*. No. 10, Society of Exploration Geophysicists (Tulsa), 2001. Chapter 1.2.

[13] B. Nicolas, J. Mars, and J. Lacoume, "Geoacoustical parameters estimation with impulsive and boat-noise sources," *IEEE Journal of Oceanic Engineering*, vol. 28, no. 3, pp. 494–501, 2003.

[14] S. M. Kay, *Modern spectral estimation, theory and application*. Signal Processing, Prentice Hall (Upper Saddle River), 1988. Chapter 6.

[15] E. C. Shang, H. P. Wang, and Z. Y. Huang, "Waveguide characterization and source localization in shallow water waveguides using the prony method," *The Journal of the Acoustical Society of America*, vol. 83, no. 1, pp. 103–108, 1988.

[16] K. M. Becker and G. V. Frisk, "Evaluation of an autoregressive spectral estimator for modal wave number estimation in range-dependent shallow water waveguides," *The Journal of the Acoustical Society of America*, vol. 120, no. 3, pp. 1423–1434, 2006.

[17] F. D. Philippe, P. Roux, and D. Cassereau, "Iterative high-resolution wavenumber inversion applied to broadband acoustic data," *IEEE Transactions on Ultrasonics, Ferroeletrics, and Frequency Control*, vol. 55, no. 10, pp. 2306–2311, 2008.

[18] F. Le Courtois and J. Bonnel, "Autoregressive model for high-resolution wavenumber estimation in a shallow water environment using a broadband source," *The Journal of the Acoustical Society of America*, vol. 135, no. 4, pp. EL199–EL205, 2014.

[19] I.-T. Lu, R. C. Qiu, and J. Kwak, "A high-resolution algorithm for complex spectrum search," *The Journal of the Acoustical Society of America*, vol. 104, no. 1, pp. 288–299, 1998.

[20] S. D. Rajan and S. D. Bhatta, "Evaluation of high-resolution frequency estimation methods for determining frequencies of eigenmodes in shallow water acoustic field," *The Journal of the Acoustical Society of America*, vol. 93, no. 1, pp. 378–389, 1993.

[21] E. J. Candès and M. B. Wakin, "An introduction to compressive sampling," *IEEE Signal Processing Magazine*, vol. 25, no. 2, pp. 21–30, 2008.

[22] N. Chapman and I. Barrodale, "Deconvolution of marine seismic data using the l1 norm," *Geophysical Journal International*, vol. 72, no. 1, pp. 93–100, 1983.

[23] P. Gerstoft, A. Xenaki, and C. F. Mecklenbräuker, "Single and multiple snapshot compressive beamforming," *arXiv preprint arXiv:1503.02339*, 2015.

[24] J. B. Harley and J. M. Moura, "Dispersion curve recovery with orthogonal matching pursuit," *The Journal of the Acoustical Society of America*, vol. 137, no. 1, pp. EL1–EL7, 2015.

[25] F. Le Courtois and J. Bonnel, "Compressed sensing for wideband wavenumber tracking in dispersive shallow water," *The Journal of the Acoustical Society of America*, vol. 138, no. 2, pp. 575–583, 2015.

[26] F. Le Courtois and J. Bonnel, "Wavenumber tracking in a low resolution frequency-wavenumber representation using particle filtering," in *International Conference on Acoustics, Speech and Signal Processing*, (Florence, Italia), pp. 6805–6809, IEEE, June 2014.

[27] P. M. Djuric, J. H. Kotecha, J. Zhang, Y. Huang, T. Ghirmai, M. F. Bugallo, and J. Miguez, "Particle filtering," *IEEE Signal Processing Magazine*, September 2003.

[28] C. Soussen, J. Idier, D. Brie, and J. Duan, "From bernoulli–gaussian deconvolution to sparse signal restoration," *Signal Processing, IEEE Transactions on*, vol. 59, no. 10, pp. 4572–4584, 2011.

[29] A. Drémeau, C. Herzet, and L. Daudet, "Boltzmann machine and mean-field approximation for structured sparse decompositions," *Signal Processing, IEEE Transactions on*, vol. 60, no. 7, pp. 3425–3438, 2012.

[30] F. Jensen, W. Kuperman, M. Porter, and H. Schmidt, *Computational ocean acoustics*. American Institute of Physics (New York), second ed., 2011. Chapter 5 and chapter 10.

[31] E. J. Candès and M. B. Wakin, "An introduction to compressive sampling," *IEEE Signal Processing Magazine*, March 2008.

[32] D. L. Donoho, "Compressed sensing," *IEEE Trans. On Information Theory*, vol. 52, no. 4, pp. 1289–1306, April 2006.

[33] B. K. Natarajan, "Sparse approximate solutions to linear systems," *SIAM Journal of Computing*, vol. 24, pp. 227–234, April 1995.

[34] S. Mallat and Z. Zhang, "Matching pursuits with time-frequency dictionaries," *IEEE Trans. On Signal Processing*, vol. 41, pp. 3397–3415, December 1993.

[35] Y. C. Pati, R. Rezaiifar, and P. S. Krishnaprasad, "Orthogonal matching pursuit: Recursive function approximation with applications to wavelet decomposition," in *Proc. Asilomar Conf. on Signals, Systems, and Computers*, 1993.

[36] S. S. Chen, D. L. Donoho, and M. A. Saunders, "Atomic decomposition by basis pursuit," *SIAM Journal on Scientific Computing*, vol. 20, pp. 33–61, 1998.

[37] R. Tibshirani, "Regression shrinkage and selection via the lasso," *Journal of the Royal Statistical Society*, vol. 58, pp. 267–288, 1996.

[38] B. A. Olshausen and D. J. Field, "Sparse coding with an overcomplete basis set: a strategy employed by v1?," *Vision Research*, vol. 37, no. 23, pp. 3311–3325, 1997.

[39] F. Krzakala, M. Mézart, F. Sausset, Y. F. Sun, and L. Zdeborová, "Statistical physics-based reconstruction in compressed sensing." available on http://arxiv.org/abs/1109.4424v2, 2011.

[40] C. Herzet and A. Drémeau, "Bayesian pursuit algorithms," in *Proc. European Signal Processing Conference (EUSIPCO)*, (Aalborg, Denmark), August 2010.

[41] M. Beal, *Variational algorithms for approximate Bayesian inference*. PhD thesis, University College of London, May 2003.

[42] F. Krzakala, A. Manoel, E. W. Tramel, and L. Zdeborová, "Variational free energies for compressed sensing," *Proc. IEEE International Symposium on Information Theory*, 2014.

[43] Y. C. Pati, R. Rezaiifar, and P. Krishnaprasad, "Orthogonal matching pursuit: Recursive function approximation with applications to wavelet decomposition," in *Signals, Systems and Computers, 1993. 1993 Conference Record of The Twenty-Seventh Asilomar Conference on*, pp. 40–44, IEEE, 1993.

[44] J. Bonnel, B. Nicolas, and J. I. Mars, "Estimation of modal group velocities with a single receiver for geoacoustic inversion in shallow water," *Journal of Acoustical Society of America*, vol. 128, August 2010.

[45] N. Barbara, J. I. Mars, and J.-L. Lacoume, “Geoacoustical parameters estimation with impulsive and boat-noise sources,” *IEEE Journal of Oceanic Engineering*, vol. 28, July 2003.